# Diffusion-Weighted Magnetic Resonance Imaging of the Prostate: Improved Robustness With Stretched Exponential Modeling

*Yousef Mazaheri, PhD,*† Asim Afaq, MD,† Daniel B. Rowe, PhD,‡ Yonggang Lu, PhD,* Amita Shukla-Dave, PhD,*† and Jarrett Grover, MS§*

**Purpose:** This study aimed to compare the intraclass correlation coefficients of parameters estimated with stretched exponential and biexponential diffusion models of in vivo diffusion-weighted magnetic resonance imaging (MRI) of the prostate.

**Methods:** After the institutional review board issued a waiver of informed consent for this Health Insurance Portability and Accountability Act–compliant study, 25 patients with biopsy-proven prostate cancer underwent 3T endorectal MRI and diffusion-weighted MRI of the prostate at 10 *b* values (0, 45, 75, 105, 150, 225, 300, 600, 900, and 1200 s/mm$^2$). The full set of *b* values was collected twice within a single acquisition. Intraclass correlation coefficients were calculated for intra-acquisition variability. From the biexponential model, the quantitative parameters diffusion coefficient (*D*), perfusion coefficient (*D**), and perfusion fraction (*f*) were estimated. From the stretched exponential model, the quantitative parameters Kohlrausch decay constant ($D_K$) and alpha ($\alpha$) were estimated.

**Results:** For the 25 patient data sets, the average intraclass correlation coefficients for $D_K$ and $\alpha$ were 95.8%, and 64.1%, respectively, whereas those for *D*, *D**, and *f* were 84.4%, 25.3%, and 41.3%, respectively.

**Conclusions:** The stretched exponential diffusion model captures the nonlinear effects of intravoxel incoherent motion in the prostate. The parameters derived from this model are more reliable and reproducible than the parameters derived from the standard, widely used biexponential diffusion/perfusion model.

**Key Words:** diffusion-weighted imaging, prostate MR imaging, intravoxel incoherent motion (IVIM), stretched exponential diffusion model

(*J Comput Assist Tomogr* 2012;36: 695–703)

In biological tissues, microscopic motion detected by diffusion-weighted imaging (DWI) includes both diffusion of water molecules, influenced by the structural components of the tissue, and microcirculation of blood in the capillary network. To separate perfusion effects from pure diffusion in diffusion-weighted magnetic resonance imaging (MRI) studies, Le Bihan et al[1–3] proposed the intravoxel incoherent motion (IVIM) biexponential model. In this model, to estimate diffusion parameters, diffusion signal was measured for a large number of *b* values, ranging from very low to high. Although it is more detailed than the monoexponential model, the biexponential model makes assumptions regarding the microcirculation and provides estimates of perfusion that are not sufficiently reproducible to be reliable.[4–6] The goal of the present study was to present an alternative approach to the multicompartment biexponential model using the Kohlrausch decay function.

Using computer simulations, Pekar et al[5] studied the precision and accuracy of biexponential parameters derived from multi–*b* value diffusion-weighted experiments to characterize perfusion and diffusion. Using model parameter values for brain, they generated noise-contaminated signal at numerous signal-to-noise ratios (SNRs). The simulations suggested that reliable estimates of perfusion coefficient, *D**, and perfusion fraction, *f*, require substantial SNRs. The simulation also indicated that SNRs need to be higher for estimation of *D** than for estimation of *f*. The substantial SNRs required for reliable estimation of biexponential parameters could potentially be achieved through averaging over regions of interest (ROIs).

One reported approach for obtaining reliable estimates of perfusion-related parameters is to hold the parameter *D** fixed.[7,8] In studying pancreatic carcinoma using multiple *b* values and the IVIM model, Lemke et al[7] set the parameter *D** to a fixed value of 20 μm$^2$/ms. A similar approach was used by Re et al[8] to generate a stable, pixel-based 3-parameter fit. Although the approach is beneficial when the goal is to enhance the contrast between the lesion and the pancreatic duct, the resultant shift in *f* values, which is an indirect consequence of changes in the actual value of *D**, limits the ability to quantitatively characterize perfusion.

If IVIM diffusion parameters are to be clinically useful, they must be robust and reliable. Here, we propose the use of the stretched exponential diffusion model to characterize IVIM diffusion signal and thus provide a measure of deviation from the monoexponential behavior caused by pseudoperfusion effects. The stretched exponential model (also referred to as the Kohlrausch decay function) was used by Bennett et al[9,10] to characterize diffusion properties of tissue at high *b* values (*b* values in the range 500–6500 s/mm$^2$). Hall and Barrick[11] explained that because the local environment of spins is thought to be nonhomogeneous, the Kohlrausch decay function is a suitable model for diffusion-weighted signal decay.

This article is organized as follows: First, we present the theoretical foundation of the stretched exponential diffusion model. Next, simulation analysis is presented to compare the precision and accuracy of monoexponential, biexponential, and stretched-exponential models. We then provide results obtained from imaging of the prostate using a previously described multi–*b* value DWI acquisition method. Finally, we compare the

From the Departments of *Medical Physics, †Radiology, Memorial Sloan-Kettering Cancer Center, New York, NY; ‡Department of Mathematics, Statistics and Computer Science, Marquette University, Milwaukee, WI; §CSM Worldwide, Inc., Mountainside, NJ.

Received for publication March 12, 2012; accepted July 26, 2012.

Reprints: Yousef Mazaheri, PhD, Departments of Medical Physics and Radiology, Memorial-Sloan Kettering Cancer Center New York, NY, (e-mail: mazahery@mskcc.org).

The authors have no conflicts of interest to report.

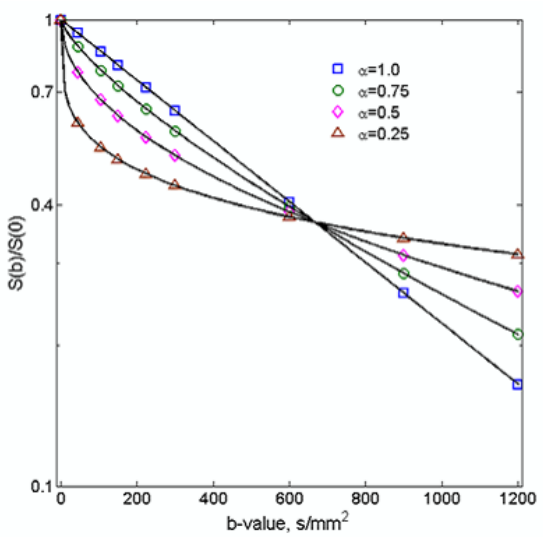


**FIGURE 1.** Representative plot of the stretched exponential function to characterize multi–*b* value diffusion signal. The value of the Kohlrausch decay function, $D_K$, was held fixed at $1.5 \times 10^{-3}$ mm$^2$/s. The value of $\alpha$ was varied between 1.0 and 0.25.

intrascan reproducibility of parameters derived with stretched exponential and biexponential models.

## MATERIALS AND METHODS

### Diffusion-Weighted MRI Data Analysis

#### Standard Monoexponential Model of Diffusion

In the simplest case, the diffusion coefficient is described by a single exponential function:

$$S(b) = S(0) \cdot exp\,(-b \cdot ADC) \qquad [1]$$

where S(b) and S(0) are signal intensities of each voxel with and without diffusion weighting, and the quantity $b$ is the diffusion-sensitizing factor (commonly referred to as the $b$ value). The apparent diffusion coefficient, ADC, is a single diffusion coefficient, which describes a multitude of diffusion properties of tissue, including both diffusion and perfusion, and is assumed to be independent of $b$ value, that is, ADC is constant.

#### Revised Model of Diffusion: Incorporating Incoherent Flow

The effect of perfusion on the total signal was modeled by taking into account the volume fraction $f$ of the water flowing through the microvessels.[3] Accordingly, the signal attenuation is given by:

$$S(b) = S(0) \cdot [(1 - f)\ exp\,(-b \cdot D) + f \cdot F] \qquad [2]$$

where $D$ is the diffusion coefficient, $f$ is the volume fraction of water in perfused capillaries, and $F$ is due to microcirculation and has a value of 1 or less that depends on capillary geometry and blood velocity.

According to a model presented by Le Bihan et al[3] perfusion can also be considered an incoherent motion, and the signal component due to microcirculation of blood is given by:

$$F = exp(-b \cdot D^*) \qquad [3]$$

where the pseudodiffusion coefficient, $D^*$, is dependent on the mean path length and blood velocity within the capillary network.

#### Stretched Exponential Model (Kohlrausch Decay Function)

An alternative approach to the multicompartment model such as the biexponential IVIM model is to use the stretched exponential model based on the Kohlrausch decay function[12]:

$$S(b) = S(0) \cdot exp\{(-b \cdot D_K)^{\alpha}\} \qquad [4]$$

where $D_K$ is the Kohlrausch decay constant. The dimensionless parameter $\alpha$ is between 0, and 1 characterizes deviation of the signal attenuation from monoexponential form. The graph of $S(b)/S(0)$ versus $\log(b)$ is characteristically stretched, (hence the alternative name of the function) and characterizes deviation of the signal attenuation from monoexponential form. The Kohlrausch function is frequently used as a purely empirical decay function, and there are theoretical arguments to justify such use.

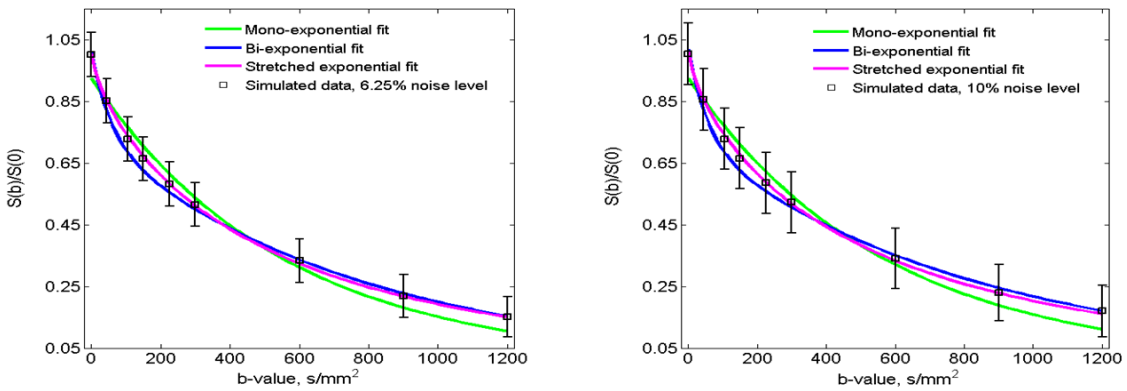


**FIGURE 2.** Plots with percentage noise at 6.25% (A) and 10% (B) levels overlaid with monoexponential, biexponential, and stretched exponential fits. The data were simulated assuming the typical in vivo signal is biexponential with parameters set to $f = 0.20$, $D = 1.5 \times 10^{-3}$ mm$^2$/s, and $D^* = 1.5 \times 10^{-2}$ mm$^2$/s. The monoexponential fitted parameters for 6.25% and 10% noise levels were ADC = $1.8 \times 10^{-3}$ mm$^2$/s and ADC = $1.8 \times 10^{-3}$ mm$^2$/s, respectively; those for biexponential fit were at 6.25% noise level, $D = 1.3 \times 10^{-3}$ mm$^2$/s, $D^* = 1.8 \times 10^{-2}$ mm$^2$/s, and $f = 0.27$, and at 10.0% noise level, $D = 1.2 \times 10^{-3}$ mm$^2$/s, $D^* = 1.8 \times 10^{-2}$ mm$^2$/s, and $f = 0.29$. The stretched exponential fitted parameters were at 6.25% noise level, $D_K = 2.0 \times 10^{-3}$ mm$^2$/s and $\alpha = 0.75$ and at 10.0% noise level, $D_K = 1.9 \times 10^{-3}$ mm$^2$/s and $\alpha = 0.73$.

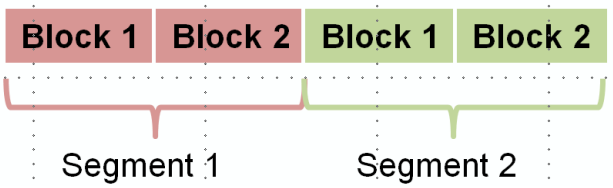


**FIGURE 3.** Multiple *b* values were acquired in a ''time-resolved'' manner during a single acquisition, alternating between low and high *b* values. This acquisition scheme permits image registration of data acquired at shorter resolved (1 TR) time intervals. A ''block'' consists of a complete set of *b* values. Each acquisition consists of 4 blocks. To assess intrameasurement variability, the 4 blocks of *b* values within a single acquisition were dividing the data into 2 data sets, or segments, each consisting of 2 blocks of data.

It is convenient as a fitting function, even in the absence of a model, given that it allows gauging in simple way deviations from the "canonical" single exponential behavior through the parameter $\alpha$ (Fig. 1).

Previous modeling of diffusion data based on the stretched exponential model was presented by Bennett et al[9,13] and more recently by Hall and Barrick.[11] In the analysis of Bennett et al,[9,13] *b* values in the range of 500 to 6500 s/mm$^2$ were used, and the stretched exponential model was presented to address deviation of the signal attenuation from monoexponential behavior. In the anomalous diffusion model of Hall and Barrick,[11] a different approach was taken to modeling a locally inhomogeneous environment; data with *b* values from 50 to 5000 s/mm$^2$ were acquired in the brain.

## Simulations

Monte Carlo (MC) simulations were performed to determine confidence in parameters derived from the analysis of alternative diffusion models. Ideal signal intensity data were generated with 9 diffusion-sensitive *b* values from 0 to 1200 s/mm$^2$ (*b* values = 0, 45, 105, 150, 225, 300, 600, 900, and 1200 s/mm$^2$). The

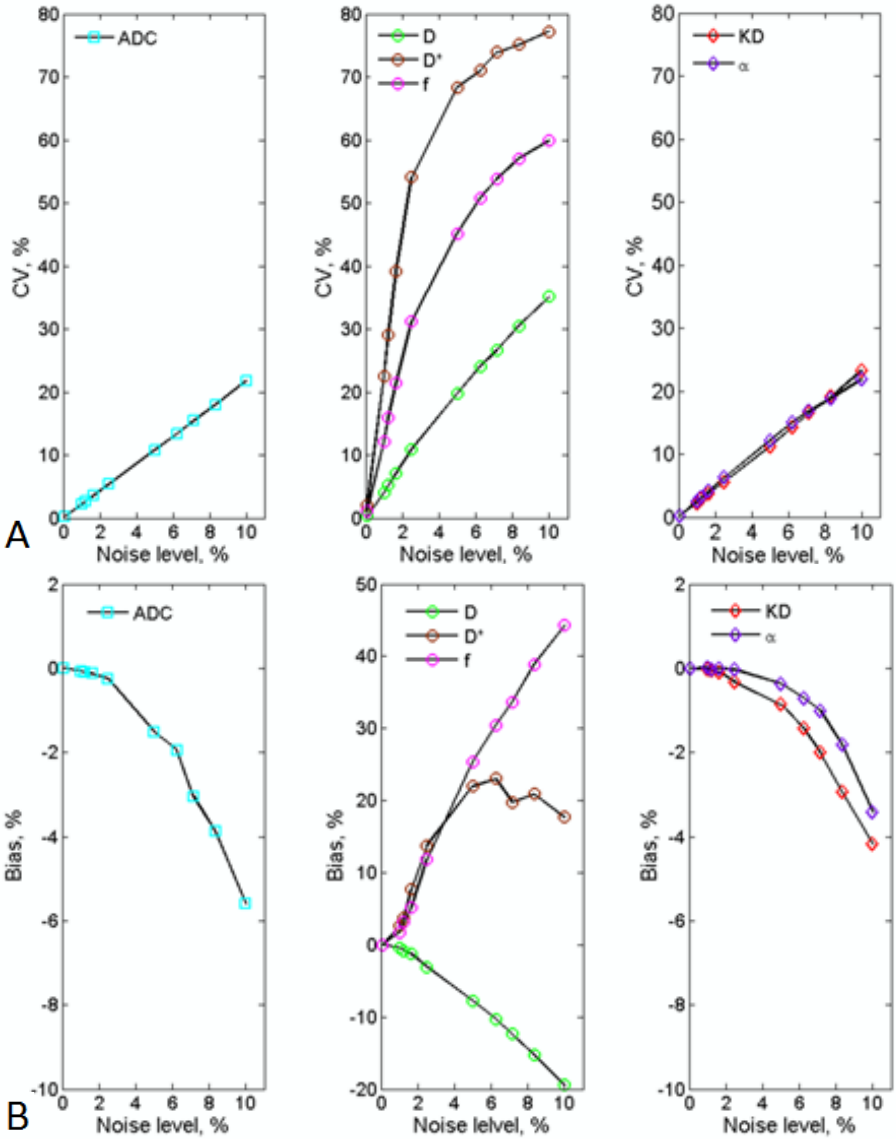


**FIGURE 4.** MC simulations of precision (CV) (A) and accuracy (bias) (B) of parameters versus percent noise of monoexponential model (ADC), biexponential model (*D**, *f*), and Kohlrausch decay function (stretched exponential) ($D_K$, $\alpha$) model.

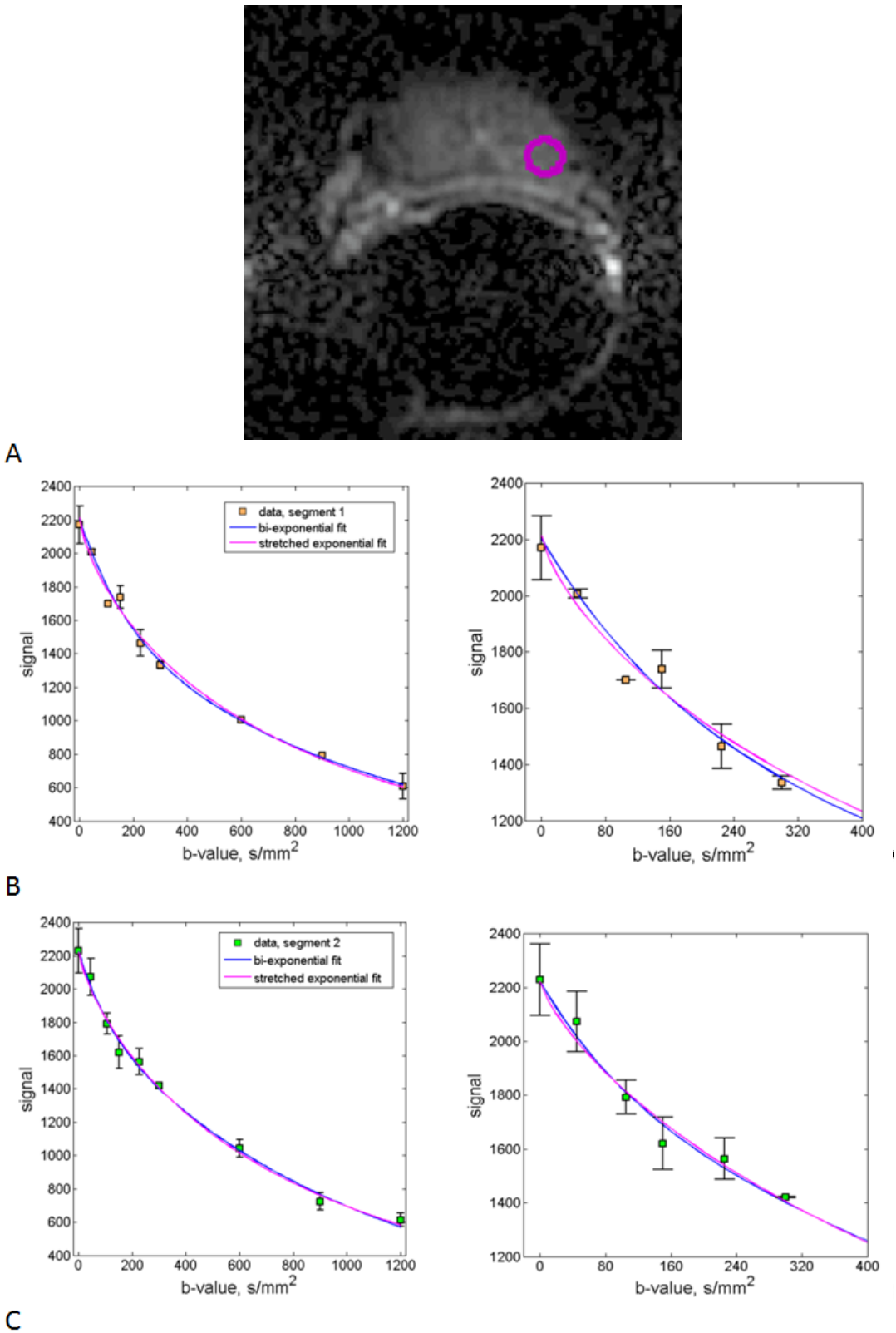


**FIGURE 5.** A, ROIs placed in the prostate shown on a $b = 0$ image. Plots of mean signal intensity (and zoomed region) and the biexponential and stretched exponential fits for the ROIs from segments 1 (B) and segment 2 (C). The parameters $D^*$, $D$, and $f$ were extracted from the biexponential model; and $D_K$ and $\alpha$, from the stretched exponential model for each segment. Biexponential model from segments 1 and 2, $D = 0.8 \times 10^{-3}$ mm$^2$/s and $1.0 \times 10^{-3}$ mm$^2$/s, $D^* = 5.5 \times 10^{-3}$ mm$^2$/s and $9.3 \times 10^{-3}$ mm$^2$/s, and $f = 0.30$ and 0.17; stretched exponential model from segments 1 and 2, $D_K = 1.2 \times 10^{-3}$ mm$^2$/s and $1.2 \times 10^{-3}$ mm$^2$/s, and $\alpha = 0.73$ and 0.77.

simulations were performed assuming that in vivo signal is biexponential, with parameters set to $f = 0.20$, $D = 1.5 \times 10^{-3}$ mm$^2$/s, and $D^* = 1.5 \times 10^{-2}$ mm$^2$/s. The values were selected based on values reported by Riches et al[6] for peripheral zone prostate ($D = 1.34$ [range, 0.69–1.92] $\times 10^{-3}$ mm$^2$/s, $D^* = 21.2$ [range, 3.89–11.00] $\times 10^{-3}$ mm$^2$/s, and $f = 0.23$ [range, 0.06–0.53]). Rician-corrupted data were generated based on method of Wiest-Daesslé et al.[14] The percentage noise is expressed as a percentage of the signal intensity at $b = 0$. For the purpose of the simulations, the percentage noise was varied from 0% to 10%. The corrupted data were fitted with monoexponential, biexponential, and stretched exponential models. Ten thousand simulations were performed at each of the 10 different noise levels, for a total of 100,000 simulations. Precision, accuracy, and normalized residual for each model were calculated. The precision of each parameter was characterized by its coefficient of variation (CV), defined as the ratio of the parameter's SD to its mean. Accuracy was assessed by the relative bias, defined as the percentage difference between the fitted and ideal parameter values. Figure 2 shows signal with noise at 6.25% and 10% levels overlaid with normalized monoexponential, biexponential, and stretched exponential fits. The models were fitted to the data with nonlinear least-squares routine using the Levenberg-Marquardt algorithm in MATLAB software (version 7.1; Mathworks, Natick, MA).

## Magnetic Resonance Imaging Data Acquisition

Our institutional review board waived the requirement for informed consent for this retrospective study, which was compliant with the Health Insurance Portability and Accountability Act. Between June 2011 and August 2011, 25 patients (age, 42–74 years) with biopsy-proven prostate cancer referred for MRI of the prostate underwent a pretreatment clinical MRI examination that included DWI. Magnetic resonance imaging was performed with a 3-T whole-body MRI unit (Discovery MR750; GE Medical Systems, Waukesha, WI) equipped with a 32-channel phased-array coil and a commercially available balloon-covered expandable endorectal coil (Medrad, Pittsburgh, PA) for signal reception.

Diffusion-weighted images were acquired using the previously described motion correction with multi–*b* value DWI technique.[15] In brief, the technique sequentially collects multiple acquisitions of 2-dimensional slices at different *b* values using a conventional single-shot spin-echo echo planar imaging acquisition with a pair of rectangular gradient pulses along 3 orthogonal axes (*x*, *y*, and *z*) simultaneously. Multiple *b* values were acquired in a "time-resolved" manner during a single acquisition, alternating between low and high *b* values. The data are collected using one or more specific sets or "blocks" of *b* values multiple times within a single acquisition (Fig. 3). Image registration using a normalized mutual information similarity measure was used to correct for spatial misalignment of diffusion-weighted volumes caused by motion. Two-dimensional affine transformation was used for motion correction.

In our study, we collected axial diffusion-weighted images with each of the following *b* values: 0, 45, 75, 105, 150, 225, 300, 600, 900, and 1200 s/mm$^2$. Four identical blocks were acquired consecutively within a single acquisition. Other parameters included repetition time/echo time (TR/TE) = 2200/88.2 milliseconds, 2 averages (or number of excitations, 2), matrix 128 × 128, field-of-view 160 × 160 mm$^2$,

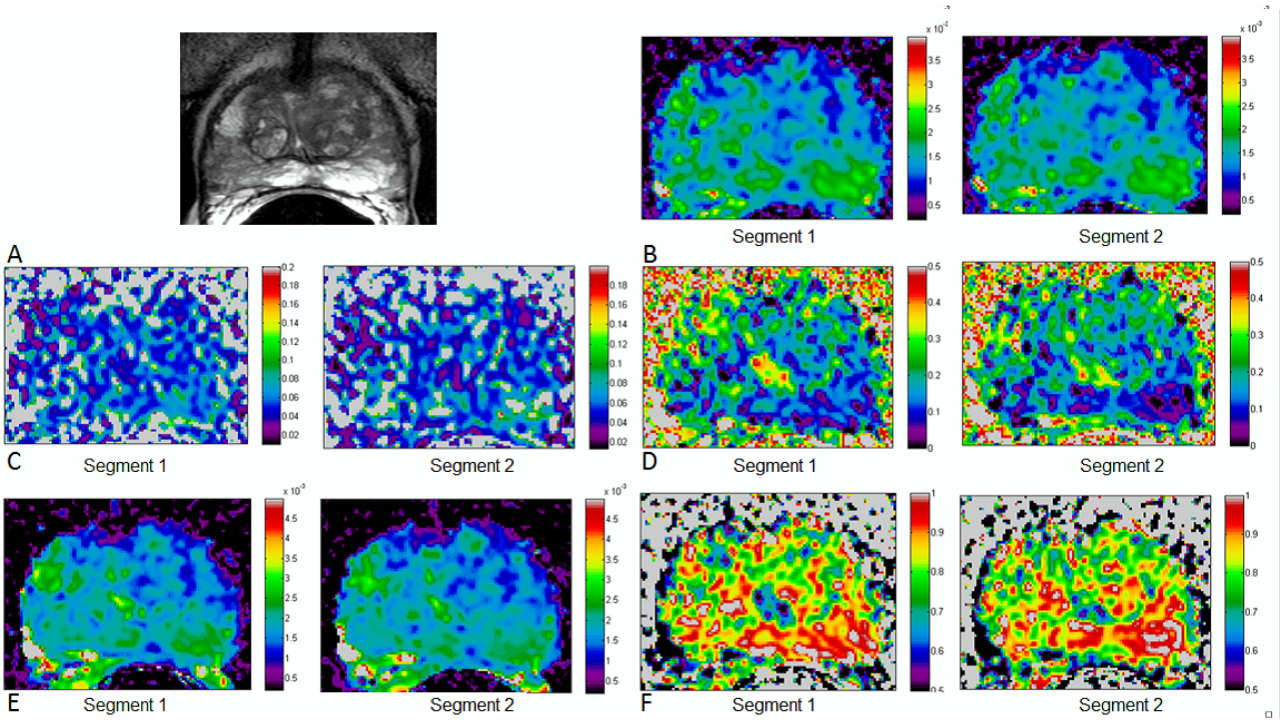


**FIGURE 6.** Representative data from a 53-year-old patient with prostate cancer, presurgical PSA level of 0.05 ng/mL, clinical stage T1c. A, Axial T2-weighted image (TR/TE = 5400/130 milliseconds). Parametric map of the biexponential parameters, *D* (B), *D** (C), *f* (D) and stretched exponential parameter $D_K$ (E) and $\alpha$ (F) and from segments 1 and 2 are shown. Diffusion-weighted image parameters were 9 *b* values, 0, 45, 75, 105, 150, 225, 300, 600, 900, and 1200 s/mm$^2$, TR/TE = 2200/88.2 milliseconds, matrix 128 × 128, field-of-view 160 × 160 mm$^2$, resolution 1.25 × 1.25 × 3 μL.

resolution 1.25 × 1.25 × 3 μL, with an acceleration factor of 2 and acquisition time of about 3 minutes. Typically, 11 to 19 sections were acquired to cover the whole prostate.

The experiments carried out in this study were intended to assess the performance of the 2 models (biexponential and stretched exponential) for IVIM signal with respect to reproducibility of the estimated parameters. To assess intrameasurement variability, the 4 blocks of $b$ values within a single acquisition were dividing the data into 2 data sets, or segments, each consisting of 2 blocks of data.

## Image Analysis

Regions of interest were drawn freehand by an experienced radiologist on one $b = 0$ image within the diffusion image series. Regions of interest were selected according to 2 criteria. The first, anatomical constraint was to select only voxels located in the peripheral zone of the prostate. The second constraint was to avoid areas containing postbiopsy hemorrhage or prostate capsule, which can result in signal abnormality on diffusion and T2-weighted images. T1-weighted images were used to detect postbiopsy intraglandular hemorrhage.[16,17]

To measure reliability of data, the intraclass correlation coefficient (ICC) was calculated to derive the data variability for the 2 consecutive acquisitions. Intraclass correlation coefficient ≤ 0.20 indicates poor agreement, 0.20 < ICC ≤ 0.40 fair agreement, 0.40 < ICC ≤ 0.60 moderate agreement, 0.60 < ICC ≤ 0.80 good agreement, and 0.80 < ICC ≤ 1.00 very good agreement. To graphically represent the relationships between measurements, scatter plots were created, and the lines of best fit were identified. The plots are intended to show agreement between parameters estimated from the first segment of data with parameters estimated from the second segment of data.

# RESULTS

## Simulations

The results of our MC simulation are shown in Figure 4. As expected, as the noise level increases, the CV and the bias in the estimated parameters increases. At the 5% noise level, the CV and bias values for the biexponential parameters were 19.7% and −7.8% for $D$, 68.3% and 22.0% for $D$*, and 45.2% and 25.3% for $f$, respectively. In comparison, for the same noise

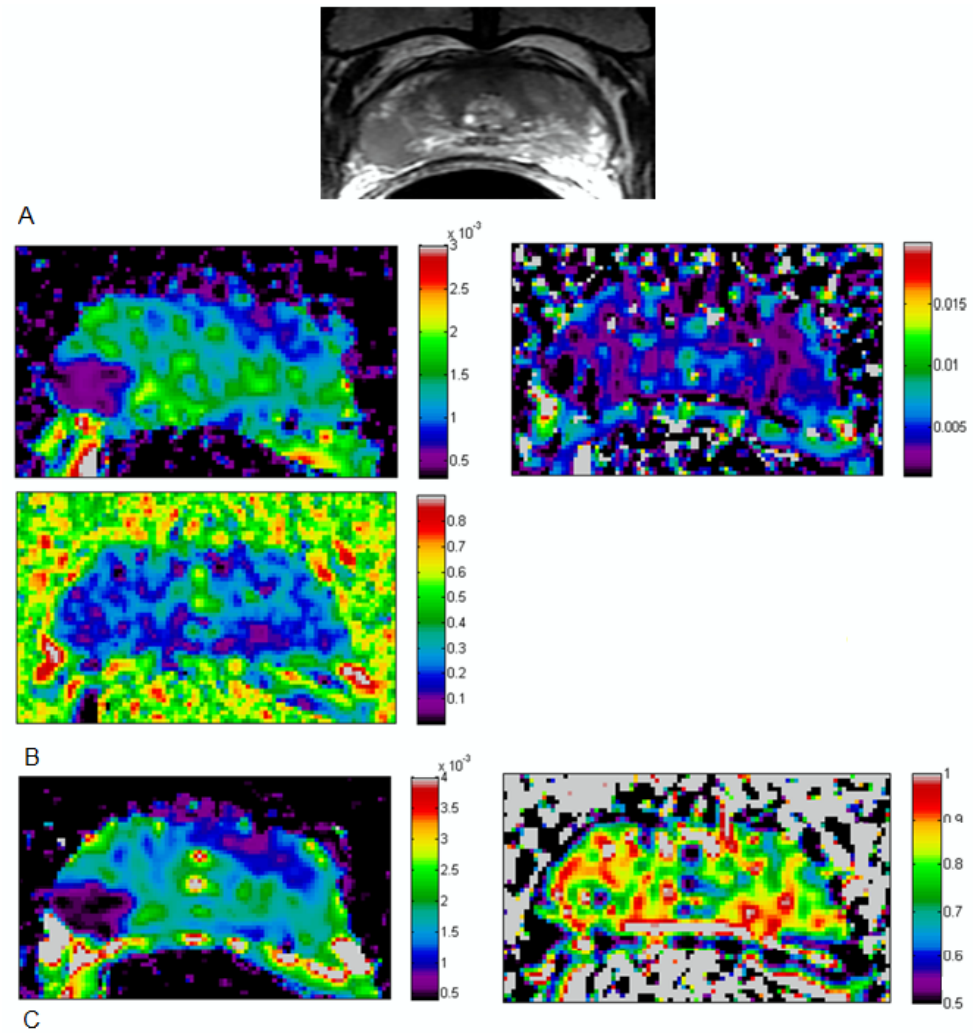


**FIGURE 7.** Representative data from a 57-year-old patient with prostate cancer, presurgical PSA level of 8.35 ng/mL, clinical stage T1c. A, Axial T2-weighted image. B, Parametric map of the biexponential parameters, $D$, $D$*, and $f$ (clock-wise). C, Parametric map for Kohlrausch decay function ($D_K$, $\alpha$) of the same slice as shown in A. Sequence parameters are identical to those used for Figure 5.

**TABLE 1.** Intraclass Correlation Coefficients Were Calculated for the Intrasession Variability for 25 Patients

| Model Parameters | ICC, % |
|---|---|
| Biexponential | |
| $D$ | 84.4 |
| $D^*$ | 25.3 |
| $f$ | 41.3 |
| Stretched exponential | |
| $D_K$ | 95.8 |
| $\alpha$ | 64.1 |

level, the values for CV and bias values for the stretched exponential parameters were 11.3% and −0.9% for $D_K$ and 12.2% and −0.4% for $\alpha$, respectively. Coefficient of variation results suggest rapidly increasing variance (low precision) for $D$, $D^*$, and $f$ in the biexponential model and variance values for $D_K$ and $\alpha$, which increase at a slower rate in the stretched exponential model. Bias results suggest increasing overestimation of $D^*$ and $f$ and underestimation of $D$ with increasing noise in the biexponential model. The underestimation of $D_K$ and $\alpha$ at the same noise level is substantially less.

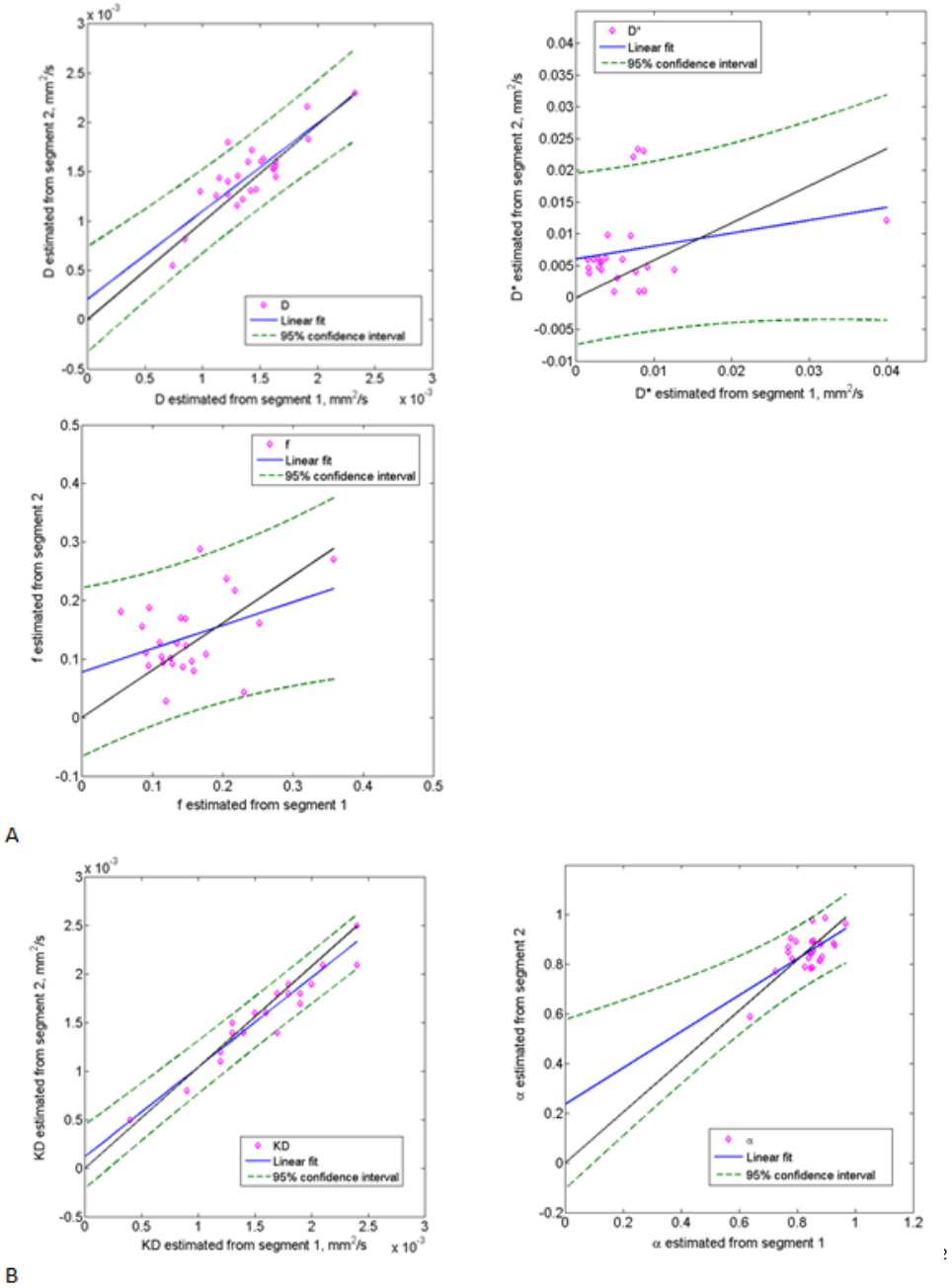


**FIGURE 8.** Scatter plots showed agreement between estimated biexponential parameters ($D$, $D^*$, and $f$) (A) and stretched exponential parameters ($D_K$, $\alpha$) (B) measured from data during the first segment with data estimated from the second segment. Identity line represents perfect agreement for data.

### Magnetic Resonance Imaging

Figure 5 shows plots of mean signal intensity and the biexponential and stretched exponential fits for the ROIs placed in the prostate shown on a $b = 0$ diffusion-weighted image from segments 1 and segment 2. Figure 6 shows the maps of the biexponential parameters ($D$, $D^*$, and $f$) (Fig. 6A) and stretched exponential parameters ($D_K$ and $\alpha$) (Fig. 6B). For each parameter, 2 maps are shown (one for each segment of the acquisition). The dynamic range was the same for the 2 segments. Overall, a comparison of the features in the $D$ and $D_K$ maps obtained in segment 1 to those obtained in segment 2 suggests that they are similar. For voxels within the prostate, $D$ values were primarily in the range of 0.0006 to 0.0026 $mm^2/s$, whereas $D_K$ values were mostly in the range of 0.0006 to 0.0032 $mm^2/s$. Variations between the 2 segments for $f$ and $\alpha$ maps were somewhat greater, although still not substantial. The $f$ values were primarily in the range of 0.0 to 0.4, and $\alpha$ values were primarily in the range of 0. 6 to 1.0. Interpretation of the variations of the $D^*$ maps is confounded by the large range of values (0.02–0.2 $mm^2/s$).

Figure 7 shows maps of the biexponential parameters ($D$, $D^*$, and $f$) (Fig. 7A) and stretched exponential parameters ($D_K$ and $\alpha$) (Fig. 7B) from a patient with biopsy-proven prostate cancer. The maps of $D$ and $D_K$ have similar features.

The ICCs for the intravariability are summarized in Table 1. Scatter plots (Fig. 8) show the level of agreement between the first segment of the acquisition and the second segment of the acquisition. The agreement between the 2 segments was poor for the parameter $D^*$. Agreement was very good for $D$ and $D_K$, moderate for $f$ and good for $\alpha$. The Pearson correlation coefficient for the biexponential parameters between the 2 segments were $r = 0.85$ for $D$, $r = 0.24$ for $D^*$, and $r = 0.41$ for $f$. In comparison, the Pearson correlation coefficient for the stretched exponential parameters were $r = 0.96$ for $D_K$ and $r = 0.64$ for $\alpha$.

## DISCUSSION

The Kohlrausch decay function, which allows the deviations from the "canonical" monoexponential function to be gauged in a simple way, is an alternative approach to biexponential modeling of IVIM signal that can provide information about diffusion and intravoxel heterogeneity simultaneously.

Our simulations demonstrated the potential advantages of the Kohlrausch decay function. First of all, parameters can be identified more precisely with this function than with the biexponential model, although this advantage seems to be reduced in high-noise situations. Second, the diffusion coefficient $D_K$ (the Kohlrausch decay constant) and $\alpha$ (a dimensionless "stretching" parameter) have a bias of less than 5% at 10% noise level. In the stretched exponential model, $D_K$ has precision similar to that of $\alpha$, and both parameters can be identified accurately: at 10% noise level, the bias is less than $-5\%$ for both of these parameters as compared with greater than 40% for $D^*$ and $-20\%$ for $D$ using a biexponential model. Bias results suggest increasing overestimation of $D^*$ and $f$ and underestimation of $D$ with increasing noise in the biexponential model. In the stretched exponential model, both parameters are increasingly underestimated at higher noise, but the degree of underestimation with increasing noise is substantially less than in the biexponential model.

Our in vivo data demonstrated that parameters estimated with the stretched exponential model are reproducible. The reproducibility of $D_K$ based on comparison of 2 segments from a single acquisition was 95.8%, which is considered excellent. The reproducibility of $\alpha$ based on comparison of the 2 segments was 64.1%, which suggests good agreement. In comparison, when the in vivo prostate data were modeled using the biexponential diffusion model, although the reproducibility of $D$ was excellent (84.4%), the reproducibility of $D^*$ was only 25.3%, indicating poor agreement, and the reproducibility of $f$ was 41.3%, indicating moderate agreement. These findings are promising because, assuming the variations are due to noise (and minimally affected by motion or other sources of variability), they suggest that parameters obtained from the stretched exponential model are robust and can serve as reliable quantitative tools. When agreement between corresponding in vivo prostate measurements was assessed, the agreement between the 2 segments was poor for the parameter $D^*$, moderate for $f$, good for $\alpha$, and very good for $D$ and $D_K$.

A major limitation of this study is that tumor ROIs were not correlated with whole-mount histopathological findings, and therefore clinical utility could not be assessed. We intend to further investigate the ability of the model to characterize tumors in the prostate when pathology maps become available after surgery. Another limitation is that we did not evaluate the variability in multi–$b$ value DWI by performing repeated measurements. In our study, the evaluation of reproducibility was limited to repeated measurements within a single acquisition. Although this analysis addresses the robustness of the methods to noise, it does not provide insight into reproducibility of variance within days (short-term) or even months (midterm). A study by Braithwaite et al[18] assessed short-term and midterm reproducibility of ADCs in DWI of the abdomen in a healthy population. Such a study is warranted with our proposed method, especially if the method is to be used as a quantitative tool for predicting and monitoring tumor response. Another limitation of our study was the small sample size. Further work is needed to establish the clinical utility of the proposed methods using whole-mount step-section pathological analysis as the reference standard.

In conclusion, we have presented an alternative model to the biexponential function to characterize diffusion and perfusion. The main advantage of the stretched exponential model is its excellent stability to noise. The disadvantage is the extension of this robustness: the model is quite rigid and may not describe data as well as other models. The parameters derived from stretched exponential model are more reliable and reproducible than the parameters derived from the standard, widely used diffusion/perfusion model.

## ACKNOWLEDGMENTS

*We are grateful to Ada Muellner, MS, for helping to edit this article and Dr. Louisa Bokacheva for the valuable discussions and technical assistance. We are thankful to Dr. Hedvig Hricak for providing support and mentorship.*

## REFERENCES

1. Le Bihan D, Turner R, MacFall JR. Effects of intravoxel incoherent motions (IVIM) in steady-state free precession (SSFP) imaging: application to molecular diffusion imaging. *Magn Reson Med*. 1989;10:324–337.
2. Le Bihan D, Breton E, Lallemand D, et al. MR imaging of intravoxel incoherent motions: application to diffusion and perfusion in neurologic disorders. *Radiology*. 1986;161:401–407.
3. Le Bihan D, Breton E, Lallemand D, et al. Separation of diffusion and perfusion in intravoxel incoherent motion MR imaging. *Radiology*. 1988;168:497–505.
4. King MD, van Bruggen N, Busza AL, et al. Perfusion and diffusion MR imaging. *Magn Reson Med*. 1992;24:288–301.

5. Pekar J, Moonen CT, van Zijl PC. On the precision of diffusion/perfusion imaging by gradient sensitization. *Magn Reson Med*. 1992;23:122–129.
6. Riches SF, Hawtin K, Charles-Edwards EM, et al. Diffusion-weighted imaging of the prostate and rectal wall: comparison of biexponential and monoexponential modelled diffusion and associated perfusion coefficients. *NMR Biomed*. 2009;22:318–325.
7. Lemke A, Laun FB, Klauss M, et al. Differentiation of pancreas carcinoma from healthy pancreatic tissue using multiple b-values: comparison of apparent diffusion coefficient and intravoxel incoherent motion derived parameters. *Invest Radiol*. 2009;44:769–775.
8. Re TJ, Lemke A, Klauss M, et al. Enhancing pancreatic adenocarcinoma delineation in diffusion derived intravoxel incoherent motion f-maps through automatic vessel and duct segmentation. *Magn Reson Med*. 2011;6:1327–1332.
9. Bennett KM, Schmainda KM, Bennett RT, et al. Characterization of continuously distributed cortical water diffusion rates with a stretched-exponential model. *Magn Reson Med*. 2003;50:727–734.
10. Bennett KM, Hyde JS, Rand SD, et al. Intravoxel distribution of DWI decay rates reveals C6 glioma invasion in rat brain. *Magn Reson Med*. 2004;52:994–1004.
11. Hall MG, Barrick TR. From diffusion-weighted MRI to anomalous diffusion imaging. *Magn Reson Med*. 2008;59:447–455.
12. Kohlrausch R. Ann Phys Chem (Poggendorff) 1854;91(179).
13. Bennett KM, Hyde JS, Schmainda KM. Water diffusion heterogeneity index in the human brain is insensitive to the orientation of applied magnetic field gradients. *Magn Reson Med*. 2006;56:235–239.
14. Wiest-Daessle N, Prima S, Coupe P, et al. Rician noise removal by non-local means filtering for low signal-to-noise ratio MRI: applications to DT-MRI. *Med Image Comput Comput Assist Interv.* 2008;11(pt 2):171–179.
15. Mazaheri Y, Do KG, Zhang J, et al. *Motion Correction of Multiple b-Values (MCMB) Diffusion-Weighted Imaging*. Toronto, Canada: 19th Meeting, International Society of Magnetic Resonance in Medicine; 2011:2990.
16. Kaji Y, Kurhanewicz J, Hricak H, et al. Localizing prostate cancer in the presence of postbiopsy changes on MR images: role of proton MR spectroscopic imaging. *Radiology.* 1998;206:785–790.
17. White S, Hricak H, Forstner R, et al. Prostate cancer: effect of postbiopsy hemorrhage on interpretation of MR images. *Radiology.* 1995;195:385–390.
18. Braithwaite AC, Dale BM, Boll DT, et al. Short- and midterm reproducibility of apparent diffusion coefficient measurements at 3.0-T diffusion-weighted imaging of the abdomen. *Radiology.* 2009;250:459–465.